CANCER BIOTHERAPY AND RADIOPHARMACEUTICALS
Volume 38, Number 1, 2023

DOI: 10.1089/cbr.2022.0023

Radiochemical Quality Control Methods for Radium-223 and Thorium-227 Radiotherapies

Abbie Hasson,[1,2] Wen Jiang,[3] Nadia Benabdallah,[2,4] Peng Lu,[1,4] Mark S. Longtine,[2] Bradley J. Beattie,[5] Lucy Summer,[2] Hanwen Zhang,[2,4,6] Richard L. Wahl,[2,6] Diane S. Abou,[2,4,6] and Daniel L.J. Thorek[1,2,4,6]

Abstract

Background: The majority of radiopharmaceuticals for use in disease detection and targeted treatment undergo a single radioactive transition (decay) to reach a stable ground state. Complex emitters, which produce a series of daughter radionuclides, are emerging as novel radiopharmaceuticals. The need for validation of chemical and radiopurity with such agents using common quality control instrumentation is an area of active investigation. Here, we demonstrate novel methods to characterize ^{227}Th and ^{223}Ra.

Materials and Methods: A radio-TLC scanner and a γ-counter, two common and widely accessible technologies, as well as a solid-state α-particle spectral imaging camera were evaluated for their ability to characterize and distinguish ^{227}Th and ^{223}Ra. We verified these results through purity evaluation of a novel ^{227}Th-labeled protein construct.

Results: The γ-counter and α-camera distinguished ^{227}Th from ^{223}Ra, enabling rapid and quantitative determination of radionuclidic purity. The radio-TLC showed limited ability to describe purity, although use under α-particle-specific settings enhanced resolution. All three methods were able to distinguish a pure from impure ^{227}Th-labeled protein.

Conclusions: The presented quality control evaluation for ^{227}Th and ^{223}Ra on three different instruments can be applied to both research and clinical settings as new alpha particle therapies are developed.

Keywords: α particle therapy, quality control, radio-thin layer chromatography, γ counter

Introduction

Radionuclides have long been used as tools to image and treat cancer. When systemically administered, specific radiopharmaceuticals may localize to sites of disease for diagnostic or therapeutic purposes. Presently, there is a growing interest in α particle emitting radiotherapy for cancer treatment. $^{223}RaCl_2$ (tradename Xofigo) is the first α particle therapy approved by the U.S. Food and Drug Administration for the treatment of bone metastatic castrate-resistant prostate cancer in men.[1,2]

Radium-223 (^{223}Ra) is a bone seeker, and it accumulates in sites of active bone turnover, as existing at metastatic

[1]Department of Biomedical Engineering, Washington University, St. Louis, Missouri, USA.
[2]Department of Radiology, Program in Quantitative Molecular Therapeutics, Washington University School of Medicine, St. Louis, Missouri, USA.
[3]Department of Biomedical Engineering, Johns Hopkins University, Baltimore, Maryland, USA.
[4]Department of Radiology, Washington University School of Medicine, St. Louis, Missouri, USA.
[5]Department of Radiology, Memorial Sloan Kettering Cancer Center, New York, New York, USA.
[6]Siteman Cancer Center, Oncologic Imaging Program, Alvin J. Siteman Cancer Center, Washington University School of Medicine, St. Louis, Missouri, USA.

Address correspondence to: Diane S. Abou; Department of Radiology, Washington University School of Medicine; St. Louis, MO 63110-1010, USA
E-mail: **dabou@wustl.edu**

Daniel L.J. Thorek; Department of Biomedical Engineering, Washington University; St. Louis, MO 63110-1010, USA
E-mail: **thorek.lab@wustl.edu**

bone tumors.[3,4] The α particles emitted by ^{223}Ra and its daughters are characterized by a very short track range, irradiating bone metastatic prostate cancer cells and the surrounding tumor microenvironment, while largely sparing healthy tissue from fatal irreversible DNA damage.[5]

Thorium-227 (^{227}Th) is also currently under investigation in clinical trials (NCT03507452, NCT03724747) for its potential in targeted α therapy. This radionuclide is the parent ion of ^{223}Ra and can be readily chelated and conjugated to various targeting vectors (Fig. 1).[6,7] This enables specific targeting of ^{227}Th to sites of soft tissue disease with molecular precision. In addition, its long half-life allows advantages for preparation, transportation, and administration.[8]

^{223}Ra and ^{227}Th are produced from an ^{227}Ac (21.7 years half-life) source and purified using an ion-exchange resin. Radionuclidic purity may be evaluated by γ-spectroscopy for subsequent labeling and radiopharmaceutical formulation.[9] However, the assortment of daughters emitted through concatenated decay of these radionuclides leads to complicated chelation status analyses and characterization of the products, which are essential for reliable quality control of these radiopharmaceutical products. In addition, the complex (γ, β-, and α-particle) decay profiles of ^{227}Th and ^{223}Ra have overlapping emission spectra, further complicating individual radionuclide distinction.[10]

Although measurement by high purity Germanium detector (HPGe) is a simple method for quality control, and ^{227}Th and ^{223}Ra are easily distinguished, many community care centers and hospitals do not possess such equipment. At present, manufacturer determination of purity, specific activity, and activity is performed at a central manufacturing or compounding site and subsequently transported to medical centers for use.

A growing consideration for the field is how to properly validate novel radiopharmaceuticals for clinical application, specifically radionuclides that produce multiple daughters and long half-lives.[11,12] In this study, a series of characterizations on technologies typically accessible for radiopharmaceutical identification and determination of purity was undertaken, including measures from radio-thin layer chromatography (TLC), γ counting, and a solid-state α-particle detector (Table 1).

^{227}Th and ^{223}Ra identification and quantification were demonstrated utilizing γ spectrometry and γ-counting and also an α-particle imaging spectrometer was evaluated. Novel use of a standard radio-TLC scanner for α-particle specific imaging was also evaluated. Through these methods, a quality control protocol for a ^{227}Th-radiolabeled protein construct was developed.

Materials and Methods

All reagents and solvents were purchased from Sigma-Aldrich, unless otherwise noted. ^{227}Th was supplied by the department of energy (Oak Ridge). All buffered solutions were prepared from metal-free water purified using Chelex

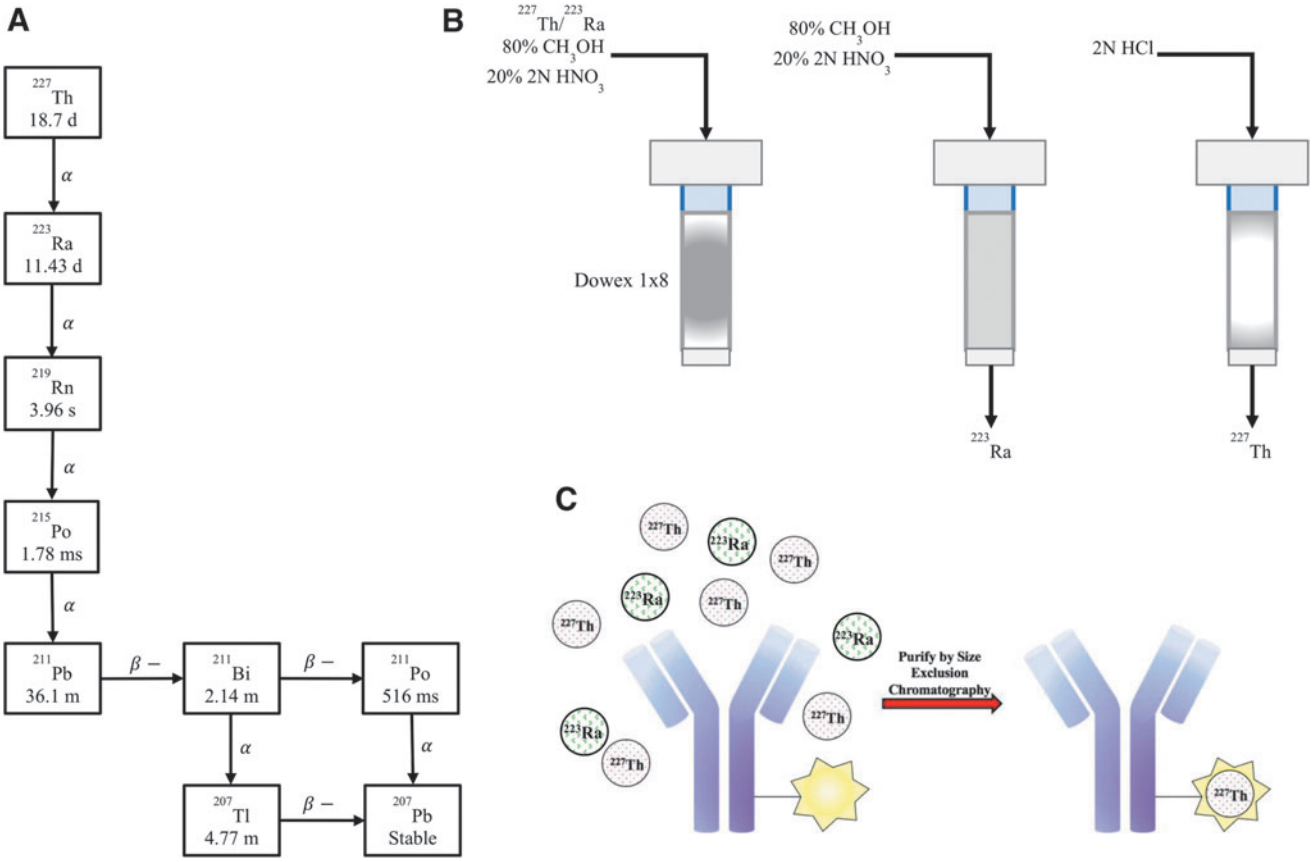

FIG. 1. **(A)** Decay chain of ^{227}Ac, which decays into ^{227}Th and ^{223}Ra. **(B)** Depiction of the anion exchange *column* used for the purification of ^{223}Ra and ^{227}Th. **(C)** Antibody radiolabeling with ^{227}Th. ^{227}Th is chelated to an antibody and purified using size exclusion chromatography.

Table 1. Most Significant α Particle Energies (Intensity >3%) of the Radioisotopes in the Decay Chain of Thorium-227 and Their Corresponding Intensities

^{227}Th		^{223}Ra		^{219}Rn		^{211}Bi		^{215}Po		^{211}Po	
Energy (keV)	*Intensity (%)*	*Energy (keV)*	*Intensity (%)*	*Energy (keV)*	*Intensity (%)*	*Energy (keV)*	*Intensity (%)*	*Energy (keV)*	*Intensity (%)*	*Energy (keV)*	*Intensity (%)*
5700.8	3.6	5433.6	1.8	6425.0	7.5	6278.2	16.2	7386.1	100	7450.3	98.9
5708.8	8.3	5539.8	8.9	6552.6	12.9	6622.9	83.5				
5713.2	4.9	5606.7	25.0	6819.1	79.4						
5756.9	20.4	5716.2	51.2								
5866.6	2.42	5747.0	8.9								
5959.7	3.0										
5977.7	23.5										
6008.8	2.9										
6038.0	24.2										

All energies are recorded in keV.

100 resin (BioRad). The handling of radioactivity requires specific caution and protection, and certification and protocol approval were provided by the Environmental Health and Safety Department at Washington University in St. Louis (Radioactive Materials Authorization 1169-01). Additional details for methods are found in the Supplementary Data, where indicated.

Characterization of ^{223}Ra and ^{227}Th using radio-TLC

Radium-223 and Thorium-227 were produced from a microgenerator, as previously described.[13] Additional details are found in the Supplementary Data. The Bioscan AR-2000 Imaging Scanner (Eckert and Ziegler Radiopharma, Inc.) was used to measure the decay of ^{223}Ra, ^{227}Th, and a mixture of both isotopes. Purified ^{223}Ra (0.025–0.1 μCi, 925–3700 Bq, 2–5 μL) was spotted in triplicate on 2.5×2.5 cm squares of Whatman paper and was not migrated (3 mm, Schleicher and Schuell).

A similar process was conducted for pure ^{227}Th and a cospotted mixture of ^{223}Ra and ^{227}Th. Each paper strip was covered in cellophane wrap and read on the radio-TLC for 1 min at a high voltage setting (1500 V) and for 5 min at a low voltage setting (1000 V). Placing each square at a similar position on the scanner, these measurements were completed daily covering an entire half-life of ^{223}Ra (11.4 days) or ^{227}Th (18.7 days), with the initial reading occurring immediately after purification.

The counts per minute (CPM) data were exported from the Bioscan software (version 3.13), and the total area under the curve was calculated using Riemann sums for each time point. The average sum was plotted and fit to a one-phase decay curve using Graphpad Prism.

Quantitative readings of ^{223}Ra and ^{227}Th using γ counting

The Wizard^2 Gamma Counter (PerkinElmer) was used to measure the decay of ^{223}Ra and ^{227}Th over an entire half-life. In brief, purified ^{223}Ra, ^{227}Th, and a cospotted mixture (0.03–0.1 μCi, 1110–3700 Bq, 1–5 μL) were pipetted on 1×1 cm squares of 3 mm Whatman paper in triplicate. Each paper was then inserted into a 12×75 mm disposable culture tube and read on the γ counter for 60 s daily. The samples were counted over the full energy window from 100 to 2000 keV.

For quantification of activity amounts, the γ-well counter and HPGe system were calibrated using a National Institute of Standards and Technology (NIST) traceable standard of ^{223}Ra. Defined volumes of the standard were aliquoted to form a dilution series, and each volume was weighed using a precision microbalance for accuracy (XP205; Mettler Toledo). The standards ranged from 0 to 9 kBq, and the full spectrum of γ-emissions was captured (2048 channels). CPM were plotted over activity, and linearity at each measured time point was $r^2 = 0.992$. The same undertaking was achieved using quantitative HPGe measurements using the 154 keV spectral line for ^{223}Ra, producing a linear response of $r^2 = 0.997$.

A method was developed to separate ^{223}Ra and ^{227}Th activity amounts using the automated sample-changing γ-counter (Fig. 2). Spectral measurements of ^{223}Ra (at secular equilibrium with its daughters) and freshly purified ^{227}Th (<10 min) were acquired daily for 25 days, providing time for ingrowth of daughter and attendant emissions. Quantitation of the ^{227}Th portion to absolute (Bq) activity amounts was made using the absolute NIST quantification of the ^{223}Ra component and the known relative amounts of each radioisotope in the mixed spectra, calculated using the Bateman equations.[14]

Taken together, these measurements allowed two basis functions (for ^{227}Th and ^{223}Ra with daughters) to be defined, each in units of counts per spectral bin per Bq. Additional details are found in the Supplementary Data.

^{223}Ra and ^{227}Th readings using Minipix α spectral detection

The Minipix spectral imaging camera (300 μm silicon; ADVACAM) was used to characterize the α decay of ^{223}Ra and ^{227}Th. Approximately 0.025 μCi (925 Bq) of purified ^{223}Ra or ^{227}Th was spotted on 3×3 cm squares of 3 mm Whatman paper. In addition, $\sim$0.025 μCi (925 Bq) of purified ^{223}Ra or ^{227}Th was spotted on a 3×3 cm square of a solid aluminum support and allowed to air dry. The clustering tool on the PIXET PRO software (ADVACAM, version 1.4.10.704) was used to collect the global cluster volume of each detection event. For the measurement of

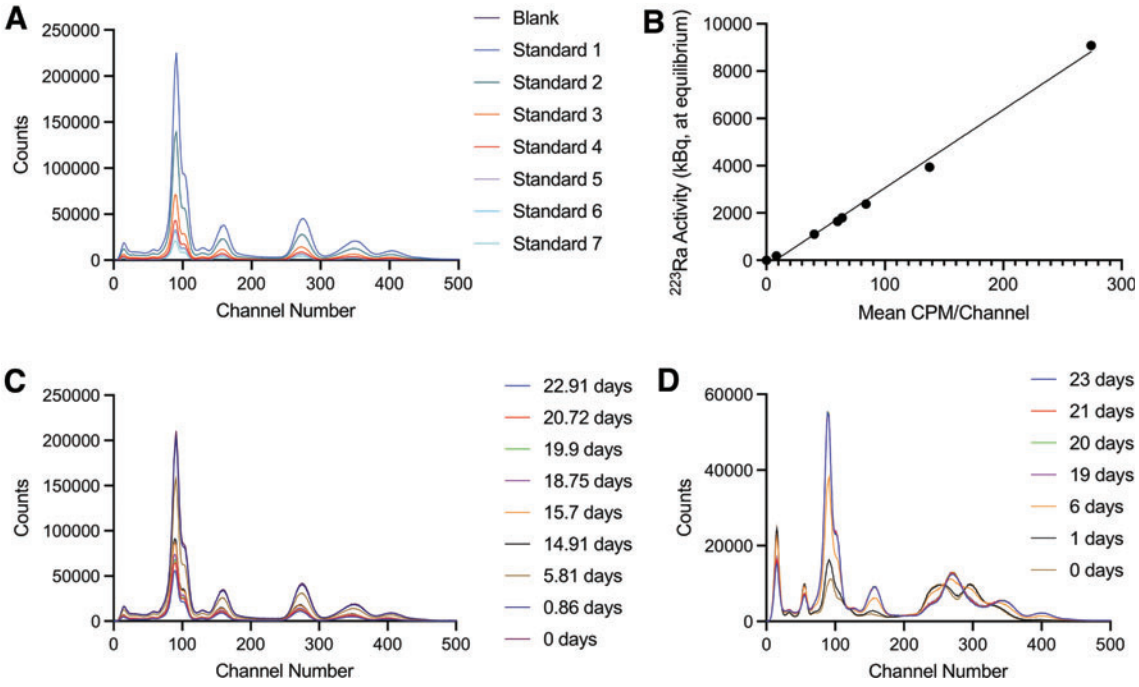

FIG. 2. **(A)** National Institute of Standards and Technology calibrated dilution series for ^{223}Ra standards. **(B)** Quantitation of activity from traceable ^{223}Ra source summed across channels. **(C)** Measurements of a ^{223}Ra source at equilibrium over time, days indicated. **(D)** Measurements of ^{227}Th over time. Ingrowth of ^{223}Ra and daughters is noted. CPM, counts per minute.

^{223}Ra and ^{227}Th α decay, samples were placed on top of the α particle imaging spectrometer, $\sim$0.7 cm from the detector, and measured daily over the period of one half-life for $\sim$15 min. The data were exported from PIXET PRO and analyzed as counts per energy bin (keV) using Graphpad Prism.

Radionuclide separation using N,N,N′,N′-tetra-n-octyldiglycolamide-coated chromatographic paper

^{227}Th (0.012 μCi, 444 Bq) and ^{223}Ra (0.007 μCi, 259 Bq) sources were cospotted on a 100 × 10 mm strip of chromatography paper impregnated with *N,N,N′,N′*-tetra-n-octyldiglycolamide (DGA; TrisKem International) and migrated in a mobile phase of 1 M HNO_3. The migrated strip was wrapped in cellophane and read using the radio-TLC under two high-voltage settings (1500 and 1000 V). Strips were measured at 5 min, 1 h, and 3 h postmigration, with an acquisition time of 5 min at 1500 V and 10 min at 1000 V. A duplicate DGA migration was separated into three equal sections and measured on the HPGe detector immediately after separation for radioisotopic identification.

^{227}Th-radiolabeled protein characterization

A protein conjugated to a ^{227}Th chelator of the hydroxypyridinone ligand (HOPO) class was purified by size exclusion spin centrifugation (Zeba column; ThermoFisher Scientific). Chelation status was analyzed by TLC before and after purification. Both purified and unpurified samples of the ^{227}Th-labeled protein were spotted in triplicate on silica chromatographic paper and migrated in a mobile phase of 50 mM diethylenetriamine pentaacetate and assessed by TLC scanner at high-voltage settings of 1000 and 1500 V. Following this reading, the strips were cut in half, and both sets were measured using the α particle imaging spectrometer. Each half was then measured on the γ counter for 60 s.

Results

The overall goal was to develop quality control methods for characterization of targeted α-particle therapy constructs. For each source purified by the microgenerator column, radioisotopic purity was evaluated using the HPGe (Supplementary Fig. S1).[13] Measurement by HPGe is a straightforward method for distinguishing ^{227}Th from ^{223}Ra, but many secondary and tertiary clinics, including academic medical centers, do not routinely use such equipment. The authors, therefore, tested the capacity of more readily available technologies to measure and report purity of an antibody-conjugated radiotherapeutic.

Radio-TLC scanner

The authors first evaluated a TLC scanner, the most widely deployed tool for radiolabeled agents, to measure the decay of ^{223}Ra and ^{227}Th using a novel α-particle specific setting. The differences in CPM acquisition for ^{227}Th and ^{223}Ra between the default high-voltage setting (1500 V) and a secondary setting (1000 V) were examined to report mixed ionizing radiation or α-particle specific emissions, respectively. A ^{227}Th source measured at 1500 V showed an increase in CPM over time, gradually stagnating in slope near its transient equilibrium (Fig. 3A). This increase in CPM

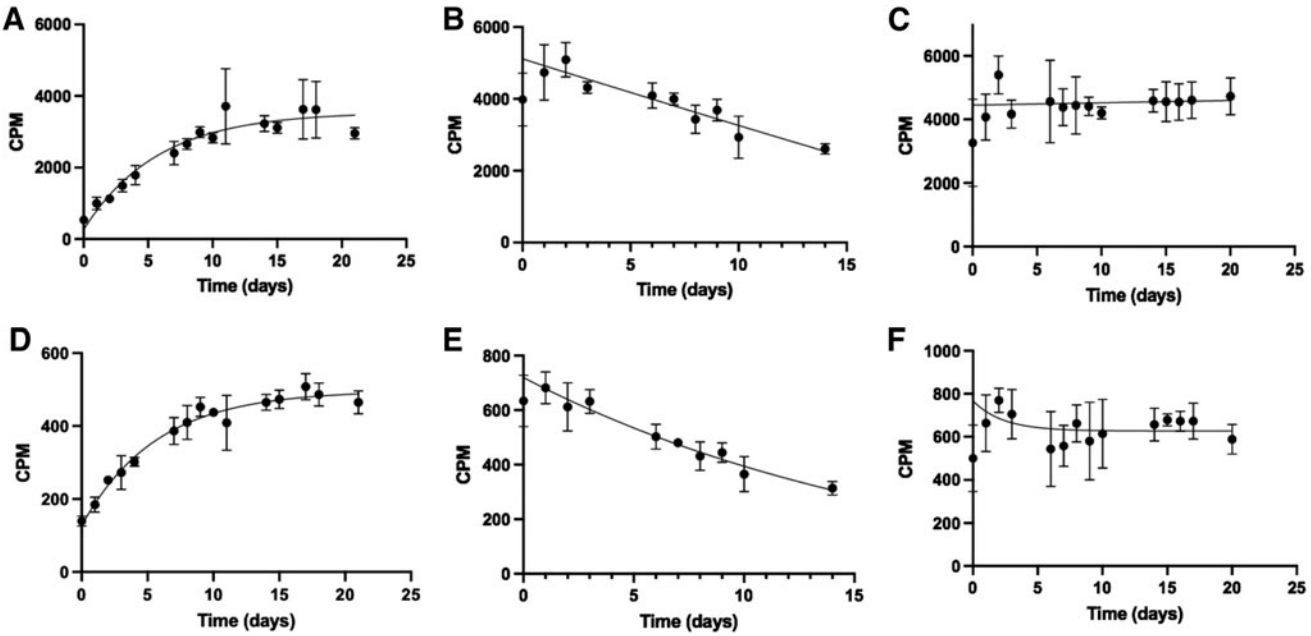

FIG. 3. Readings at 1500 V **(A–C)** and at 1000 V **(D–F)** of each radioisotope and a mixed source spotted on cellulose support, measured over time. **(A, D)** ^{227}Th CPM were plotted and fit according to a one-phase exponential decay. **(B, E)** ^{223}Ra CPM were plotted and fit to a one-phase exponential decay. **(C, F)** Mixed source of ^{223}Ra and ^{227}Th. For all curves, the initial point is excluded from the exponential fitting to allow the system to reach equilibrium. *Error bars* indicate standard deviation between triplicates. CPM, counts per minute.

over time can be attributed to the ingrowth of its daughter isotopes, specifically ^{223}Ra.

Measured under similar parameters, ^{223}Ra showed a profile moderately fitted over a standard one-phase decay ($r^2 = 0.5810$; Fig. 3B). This poor fit is most likely due to the ingrowth of ^{223}Ra daughters. The cospotted mixture of ^{227}Th and ^{223}Ra produced a fitted curve with minimal changes in CPM over the half-life of ^{227}Th (Fig. 3C), again demonstrating the limitations of the system in measuring an isotopic mixture.

At lower bias voltage, β-particles will not produce detectable ionization events, whereas higher energy α-particles will produce electrons suitable for signal amplification, allowing for α-particle specific readings at 1000 V (Fig. 3D–F). The observed curve profiles were similar at 1000 and 1500 V for the mixture of ^{227}Th/^{223}Ra and for ^{227}Th alone. However, the count plot for ^{223}Ra matched a more accurate one-phase decay despite the presence of daughters ($r^2 = 0.8611$).

The authors were interested to see how these results would compare with measurements of a migrated TLC strip separating ^{223}Ra from ^{227}Th using the default and α particle specific settings. DGA-impregnated TLC paper was used to separate ^{227}Th from ^{223}Ra by ionic discrimination. Immediately after migration, three distinct peaks were recorded at the 1500 V setting (Fig. 4A), whereas two peaks were present when measured at 1000 V (Fig. 4D). Approximately 1 h later, the middle peak had decreased significantly (Fig. 4B), and by 3 h postmigration, this peak disappeared (Fig. 4C). The peaks at the front and base of the strip were not observed to decrease over this timeframe.

To verify the radioisotopic identity of each peak, a second strip was migrated, and each section was measured using the HPGe detector (Supplementary Fig. S1D–F). These measurements suggested that [^{227}Th]Th^{4+} remained at the bottom of the strip, [^{223}Ra]Ra^{2+} migrated to the top, and ^{211}Bi (3+ charge) (half-life = 2.14 min) was present in the middle. Based on these results, the radio-TLC has a limited ability to quantitatively describe ^{227}Th and ^{223}Ra, although the 1000 V setting enhances resolution and increases the accuracy of measurements.

Sodium iodide γ counting

Another widely available instrument for radiopharmaceutical quality control is the γ-counter. Although highly sensitive to γ emissions, distinction of ^{227}Th and ^{223}Ra is challenging due to overlapping emissions (Supplementary Fig. S2A). The CPM acquired over a full window of energy spectra (100–2000 keV) for ^{227}Th and ^{223}Ra across all channels (open window) presents similar measurement profiles to those acquired under the radio-TLC scanner (Fig. 5A, B). The mixture of the two radioisotopes on the γ-counter shows a trend that is somewhat similar to that of ^{227}Th (Fig. 5C). This is because a higher activity of ^{227}Th than ^{223}Ra was initially spotted on the paper.

To use this ubiquitous tool for radiopharmaceutical evaluation of ^{227}Th and ^{223}Ra, a method to deconvolute each energy spectrum was developed and the counts to report activities for each radioisotope were calibrated, enabling absolute quantification (Supplementary Fig. S2B). The method was tested by measuring an initially pure ^{227}Th sample. In this study, a highly accurate one-phase decay curve ($r^2 > 0.99$) was observed while separately recording the ingrowth of ^{223}Ra (Fig. 5D).

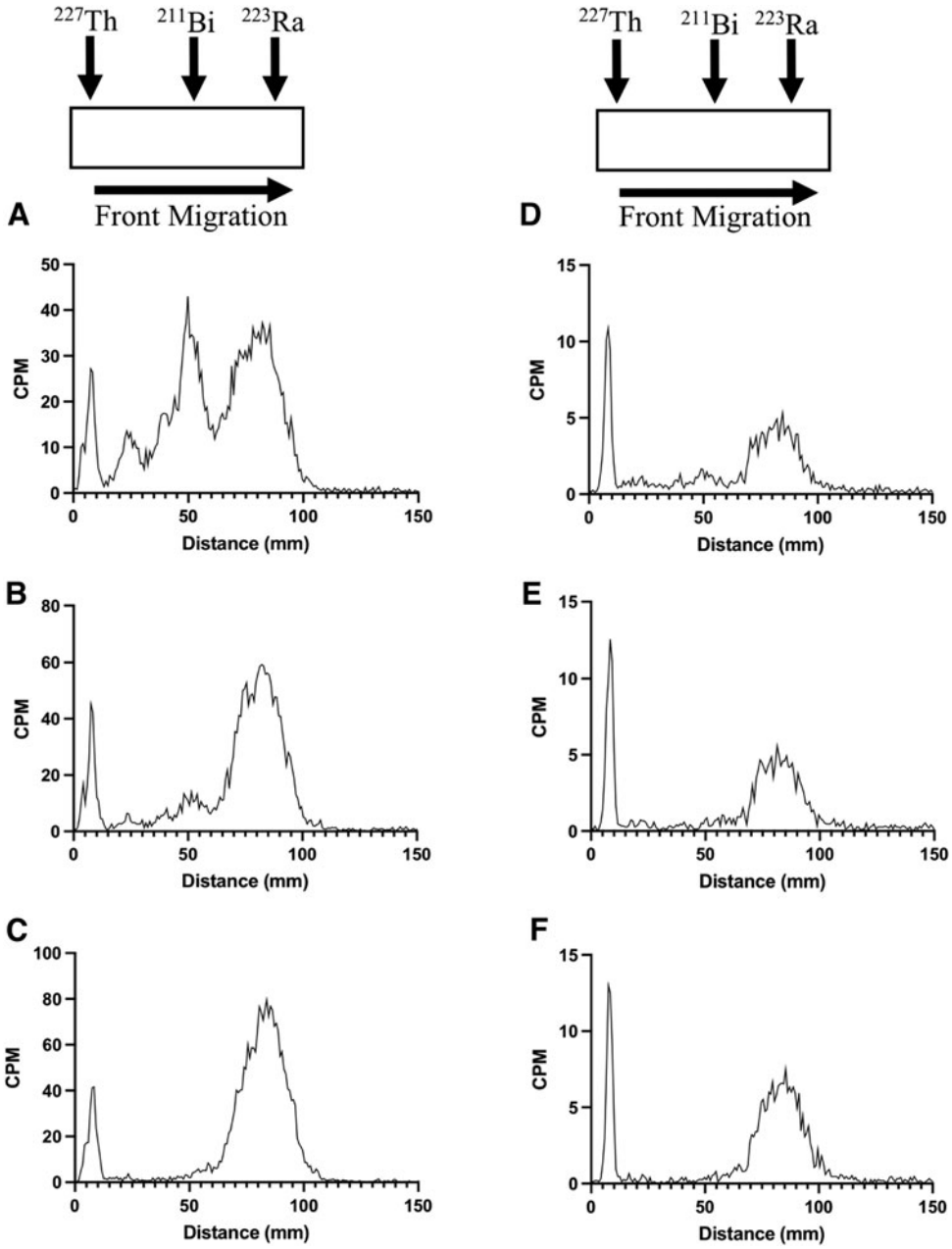

FIG. 4. A strip of DGA-coated chromatographic iTLC paper was spotted with a mixture of ^{223}Ra/^{227}Th at 10 mm and migrated with a mobile phase of 1 M HNO_3 up to 100 mm. TLC readings over high voltage 1500 V at 20 min **(A)**, 1 h **(B)**, and 3 h postmigration **(C)**. TLC readings of the same mixture at 1000 V at 5 min **(D)**, 1 h **(E)**, and 3 h postmigration **(F)**. The *middle peak* seen at both high-voltage settings immediately after purification gradually decreases until it completely disappears 3 h postmigration. CPM, counts per minute; DGA, *N,N,N′,N′*-tetra-n-octyldiglycolamide; iTLC, instant thin layer chromatography; TLC, thin layer chromatography.

As expected, pure ^{223}Ra reveals the predicted one-phase decay ($r^2 > 0.99$; Fig. 5E). The profiles of ^{227}Th and ^{223}Ra in the cospotted mixture showed the expected exponential decay for ^{227}Th while recording ^{223}Ra ingrowth (^{227}Th: $r^2 = 0.9294$; Fig. 5F). Together, this evaluation demonstrates the utility of this method to reliably separate the ^{223}Ra and ^{227}Th γ spectra to quantitate activities accurately.

α *Particle spectral detection*

^{227}Th and ^{223}Ra emit α particles at characteristic energies, and isotope identification based upon these high-energy particles can be used for radiopharmaceutical evaluation. The authors were interested to use the Minipix spectral imaging camera for this purpose, a robust and mobile system for localized α-particle detection (Table 2). The α spectra of pure ^{227}Th and ^{223}Ra were evaluated and it was found that they were significantly different, allowing for differentiation between the two (Fig. 6F).

Qualitatively, ^{223}Ra shows two very spread peaks at ~5500 and 7500 keV (Fig. 6B). The peak seen at 5500 keV corresponds to the α particles that are released by ^{223}Ra (Table 2). The higher energy α-particles are most likely contributed by the daughters of ^{223}Ra, specifically ^{215}Po (7386.1 keV) and ^{210}Po (7450.3 keV) and energies are collated in Table 2. Over 13 days, total counts in the ^{223}Ra sample peaks decreased by approximately one half, corresponding to its half-life (Fig. 6E).

Unlike ^{223}Ra, pure ^{227}Th showed a single distinct peak at ~5500 keV (Fig. 6C). Over time, the counts of this peak increase (Fig. 6D), due to ^{223}Ra ingrowth, which emits α particles close in energy (Table 2). The emergence of a

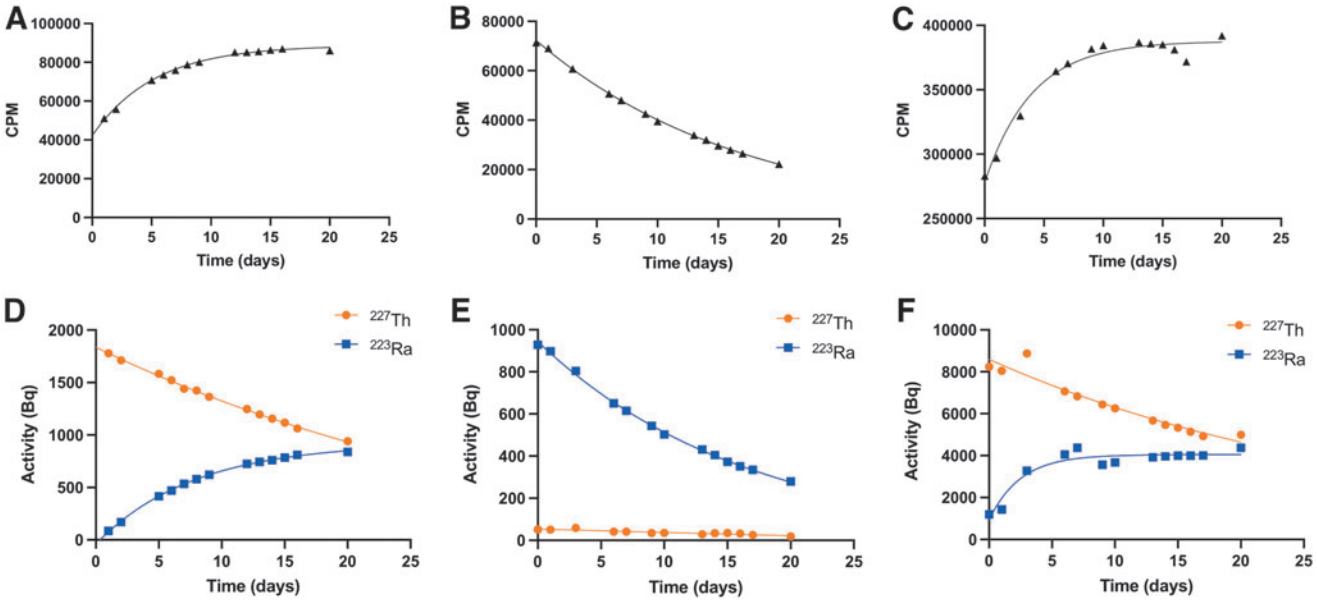

FIG. 5. Total CPM acquired in an open window channel measured for ^{227}Th **(A)**, ^{223}Ra **(B)**, and a mixture **(C)**; Deconvoluted activity (Bq) calculated for a pure ^{227}Th sample **(D)** showing ^{227}Th decay fitting a single-phase decay ($R^2 = 0.9980$), as well as ^{223}Ra ingrowth. **(E)** Activity (Bq) for ^{223}Ra fit with a single-phase decay ($R^2 = 0.9986$). **(F)** ^{227}Th and ^{223}Ra mixed sample activity (Bq) plot. CPM, counts per minute.

TABLE 2. SPECIFICATIONS FOR INSTRUMENTATION EXAMINED IN THESE METHODS

	Bioscan—1500 V	*Bioscan—1000 V*	*γ Counter*	*Minipix*
Detected radiation	All ionizing radiation	α particles	γ	All ionizing radiation
Detection mechanism	P-10 ionizing gas	P-10 ionizing gas	Well-type NaI detector	Si solid-state semiconductor (256 × 256 pixels)
Detection time[a]	1 min	5 min	1 min	15 min
Detection resolution	3 mm[b]	3 mm[b]	<30%[b]	Spatial: 9 lp/mm Energy: 0.8 keV (THL) and 2 keV (ToT)
Software	WinScan	WinScan	Wizard[2] data analyzer	PixetPRO
Portable	No	No	No	Yes

[a]For samples >0.025 μCi.
[b]For most γ emitters.
THL, threshold level; ToT, time-over-threshold.

second peak at 7500 keV again corresponds to the high energy α particles emitted by the daughters of ^{223}Ra.

The activity spotted on Whatman paper demonstrated low-energy resolution of individual α-particle spectra. This may be due to attenuation in air, by the required chromatography support and angular dispersion. Acquisitions were not collimated, as it produced no significant reduction in the energy distribution of individual peaks (not shown). When a pure ^{223}Ra or ^{227}Th source was spotted on a solid aluminum support, however, the energy resolution increased significantly (Fig. 6G). Here, comparative assessment of α-spectral detection permitted the differentiation of ^{227}Th and ^{223}Ra.

^{227}Th-radiolabeled protein quality control

The previously presented analytical methods were applied to characterize a purified and nonpurified ^{227}Th-radiolabeled protein. After migration on silica-coated chromatography paper, samples were first measured by radio-TLC. For the purified sample, only a single peak at the base of the strip was read, while the unpurified sample presented two peaks, suggesting the presence of free radioisotopes (Fig. 7A, B, E, F). These results demonstrate the value of the radio-TLC to evaluate the purity of a sample after it is migrated by TLC, but also its inability to identify specific radionuclides.

The authors next measured the ^{227}Th-radiolabeled protein using the γ counting protocol on a bisected sample. The purified protein showed only ^{227}Th, which was present primarily at the bottom of the TLC strip; this contrasts to the unpurified material for which the majority of activity at the front was identified as ^{223}Ra (Fig. 7C, G). The radiolabeling efficiency (92%) and radiochemical purity (>98%) for the purified compound were significant. The samples were also

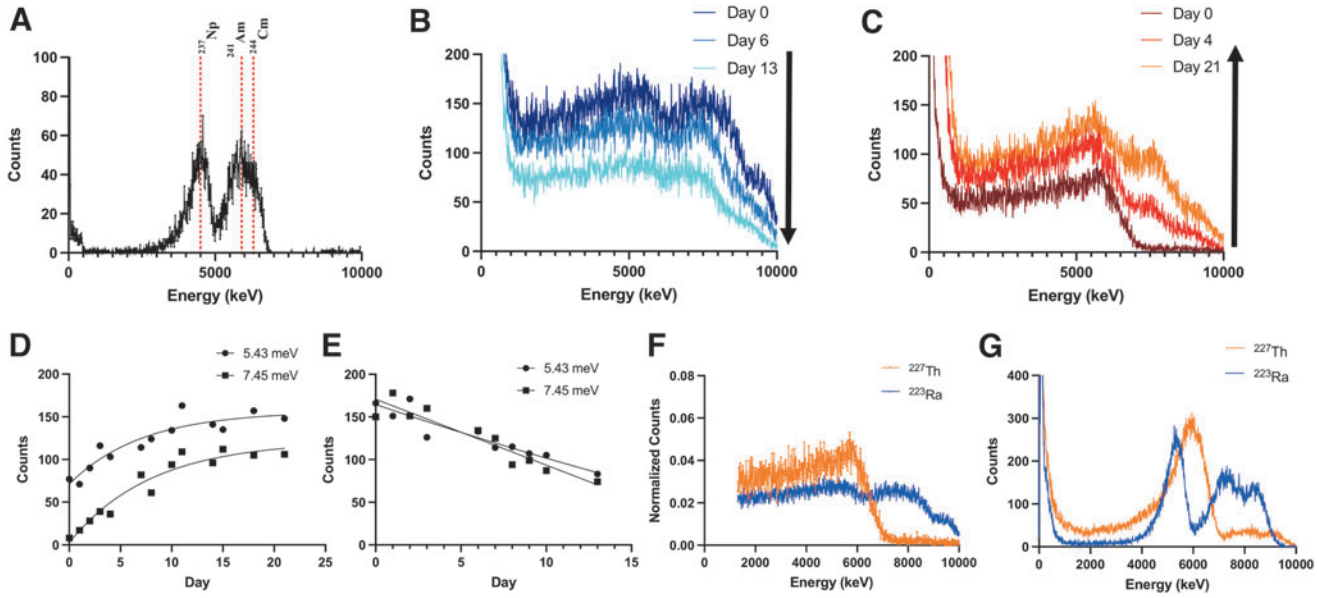

FIG. 6. **(A)** A ^{241}Am/^{237}Np/^{244}Cm standard source read using Minipix spectral imaging camera. From *left* to *right*, the three peaks correspond to the α-particles emitted by ^{237}Np, ^{241}Am, and ^{244}Cm. **(B, C)** ^{223}Ra and ^{227}Th imaging spectra over one complete half-life. **(D, E)** Plotted counts acquired at 5.43 and 7.45 MeV for pure ^{227}Th **(D)** and ^{223}Ra **(E)**. 5.43 MeV depicts the most significant α particle contribution emitted by ^{223}Ra, and 7.45 MeV corresponds to the α particle released by ^{211}Po and relates to the second peak seen in the graphs. Both increase over time for ^{227}Th and decrease for ^{223}Ra. **(F)** For the mixed spectra, the day 0 measurements of the radionuclides from **(B)** and **(C)** were normalized and plotted together. **(G)** The α spectra of ^{227}Th and ^{223}Ra plus daughters when spotted on an aluminum support.

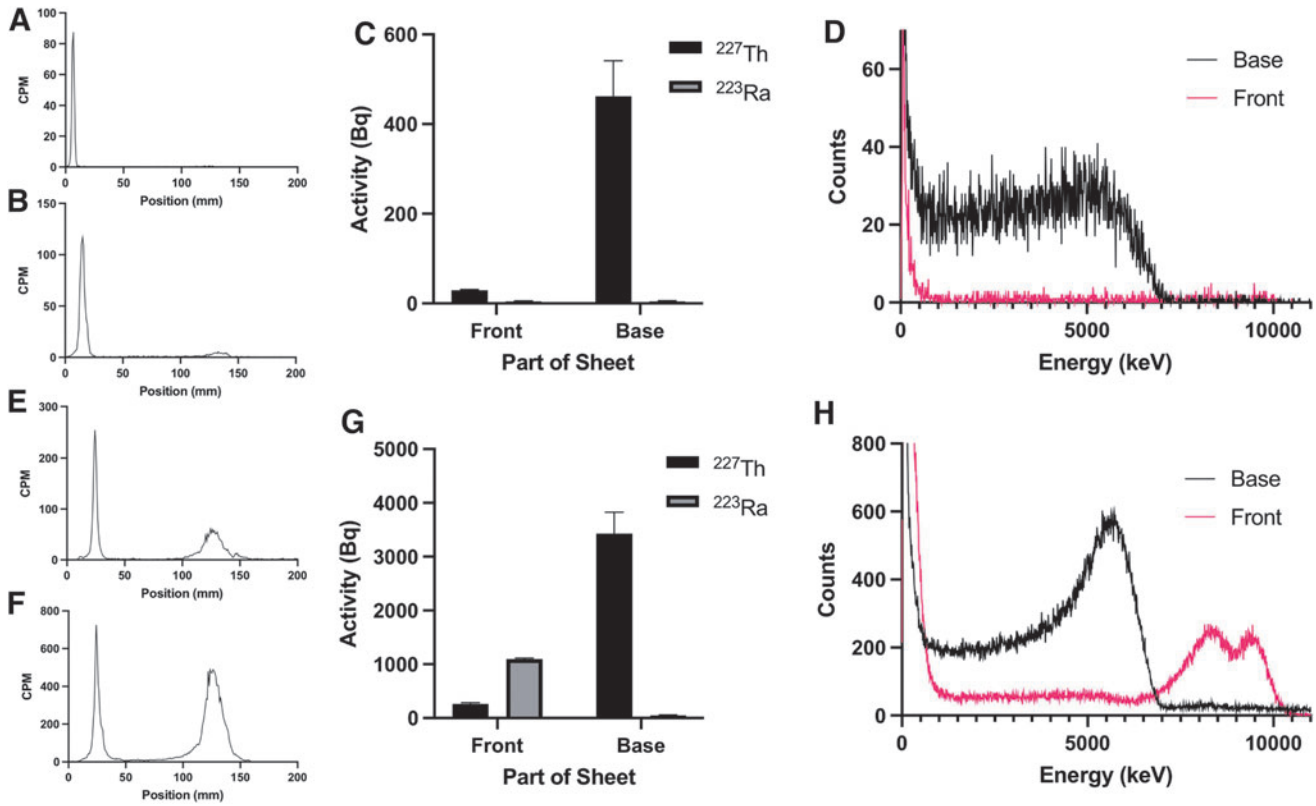

FIG. 7. ^{227}Th-labeled antibody migrated on silica-coated chromatographic iTLC with DTPA (10 mM). Purified **(A–D)** and nonpurified **(E–H)** material were compared using radio-TLC scanner **(A, B, E, F)**, γ counting **(C, G)**, and α spectral imaging **(D, H)**. The TLC scanner of purified and nonpurified ^{227}Th-labeled protein was acquired immediately after migration at a high-voltage setting of 1000 V **(A, E)** and 1500 V **(B, F)**, showing a main peak at the spotted area characteristic of ^{227}Th-labeled material and migration of unchelated ^{223}Ra at the *top* of the strip. **(C, G)** Purified **(C)** and unpurified **(G)** ^{227}Th-labeled protein measured using γ counting. ^{227}Th was found primarily nonmigrated at the *bottom* of the strip, confirming protein labeling. ^{223}Ra was detected at the *top* of the strip for the unpurified material **(G)**; **(D, H)** α spectral imaging of the purified **(D)** and nonpurified **(H)** ^{227}Th-labeled antibody showed ^{227}Th α emission at the *bottom* of the strip for both materials and ^{223}Ra contribution at the *top* of the strip for the nonpurified material. CPM, counts per minute; DTPA, diethylenetriamine pentaacetate; iTLC, instant thin layer chromatography; TLC, thin layer chromatography.

read on the Minipix spectral imaging camera. The purified sample depicts ^{227}Th at the origin with nothing detected at the solvent front. Conversely, the unpurified sample reveals ^{223}Ra at the front of the strip (Fig. 7D, H).

Discussion

The ability to accurately analyze a radiolabeled pharmaceutical is critical in both development and translation of new radiopharmaceuticals. With increasing interest in the field of radiopharmaceuticals for therapeutic use, the classical instrumentation utilized for radiotracer evaluation may be insufficient to assess the purity of agents that involve concatenated decay products with complex emission profiles.[3,13] The evaluation of several technologies was conducted to determine the capacity of widely available or affordable systems for these purposes. These results demonstrate the ability to quantitatively discriminate between ^{227}Th and ^{223}Ra utilizing a γ-counter, as well as the practical applications of these methods for the quality assessment of radiolabeled antibodies.

One common quality control approach for radiopharmaceutical evaluation is TLC migration read using a P-10 gas imaging scanner. The system is, by manufacturer default, operated at a setting of 1500 V. These results show that at 1500 V, the imaging scanner presents low sensitivity for measuring the decay of complex emitters. The measured decay of ^{223}Ra presented an r^2 of only 0.5810 to an exponential fit. This is likely explained by the presence of its daughters, which emit X-rays, γ-rays, electrons, and α-particles for which the system has variable sensitivities.

The same observation is noted for pure ^{227}Th, which did not follow a one-phase decay. This increase in signal before equilibrium can be explained by the ingrowth of ^{223}Ra, which presents a comparable half-life (11.4 days) and strong emitted γ rays (324 keV, 3.64%; 269 keV, 13.30%; 154 keV, 6.02%; 144 keV, 3.47%) and has increased detection through ionization of the P-10 gas source. When lowering the high-voltage setting to 1000 V, the authors found that the accuracy of measurement increased substantially for ^{223}Ra ($r^2 = 0.8611$).

A different migration profile was recorded for a mixture of ^{223}Ra and ^{227}Th when the scanner was used at a setting of 1500 V as compared to at 1000 V. At the lower voltage setting, the spatial resolution of peaks was enhanced, at the cost of longer acquisition duration. As both time and resolution are important considerations, the application of the radio-TLC will determine which high-voltage setting is appropriate. These observations suggest the limitations of the imaging scanner to quantitatively describe complex emitting isotopes, but the utility is apparent in qualitatively determining impurities in a migrated sample.

The total counts obtained from γ-counting readings under an open energy window setting (100–2000 keV) showed similar results to those of the radio-TLC. However, ^{223}Ra values demonstrated an accurate one-phase decay ($r^2 = 0.9993$). This increase in accuracy when read on the γ-counter is due to the selective measurement of γ-rays. The γ-energy spectra of ^{227}Th and ^{223}Ra share significant regions of overlap and are, therefore, challenging to distinguish. Measurements of each pure radioisotope presented classical one-phase decay with time, with an $r^2 > 0.99$ for both ^{227}Th and ^{223}Ra sources over the course of 20 days. Both the mixture and pure ^{227}Th capture the ingrowth of ^{223}Ra.

The absolute activity values first begin to plateau $\sim$15 days postpurification, consistent with the transient equilibrium (19 days). The deconvolution method employed here enhances the quantification capabilities of the γ-counter, enabling the distinction of ^{227}Th from ^{223}Ra and can be applied in research or clinical settings for purity assessment as well as an exact activity amount of each isotope in a mixture. This method may be useful for clinical quality control applications, which currently employ high-resolution γ-spectroscopy.[15]

As another analytical method for measuring the emitted α-particles from ^{227}Th and ^{223}Ra, detection using the Minipix solid-state semiconductor was investigated. The results show that this method was also able to differentiate between ^{227}Th and ^{223}Ra. Pure ^{227}Th can be isolated by a single peak close to 6000 keV, which is consistent with the reported α particles (Table 2). Over time, the main peak observed shifts slightly downward in energy and increases in counts as ^{223}Ra grows into the mixture, and a second peak closer to 8000 keV appears.

This second high-energy peak becomes apparent in as little as a day postpurification, demonstrating the utility of this method to differentiate between pure and impure ^{227}Th. Pure ^{223}Ra measured over time shows two peaks, with the lower peak corresponding to ^{223}Ra and the upper peak to its higher energy α-emitting daughters. Both peaks decrease in overall counts over the course of one half-life to approximately half that of the day 0 measurement, consistent with the natural decay of the radioisotope. As demonstrated here, it is possible to qualitatively measure and distinguish ^{227}Th and ^{223}Ra by α-spectrometry.

The authors did observe significant spreading of individual peaks when measuring both ^{227}Th and ^{223}Ra. The high number of emitted α-particles (Table 2) and the distance that the α-particles must travel through the air before reaching the detector (0.7 cm) contribute to this observation. Using an aluminum support in place of the filter paper improved the energy resolution of ^{223}Ra and ^{227}Th samples. This implies the dispersion of α-particle energies was due to absorption within the paper. From these results, the authors note that a solid support may provide improved α-particle spectrometry-based assessment of radiopharmaceuticals.

Finally, the practicality of these methods using a ^{227}Th-labeled protein drug was shown, and the important clinical applications of this study for other radiopharmaceutical products incorporating complex emitters were demonstrated, such as ^{223}Ra and ^{225}Ac, among others. The authors showed the ability to distinguish between the purified and nonpurified construct utilizing all three previously described methods. The radio-TLC at both high-voltage settings clearly demonstrates the presence of two chemically different species in the unpurified sample, but the authors were unable to identify individual radioisotopes by TLC evaluation.

To further characterize each sample, the upper and lower sections of the TLC strip were measured using the γ-counter and the counts per channel of energy were processed using

the deconvolution method. The activity of ^{227}Th and ^{223}Ra in each sample was quantified, and the authors determined that the majority of the impurity that migrated to the front of the strip in the unpurified sample was free ^{223}Ra. This is a validation of the γ-counting method to quickly and accurately determine the purity of a prepared radiopharmaceutical. The final results were confirmed by α-spectral analysis and HPGe measurement.

A final consideration is the improvements that these methods can make to current quality control practices. Currently, measurement by HPGe is the gold standard for discrimination between ^{227}Th and ^{223}Ra. However, this equipment is expensive and not accessible at all research and care facilities, and these methods propose three instruments that are widely available. With the exception of the γ-counter, the instruments are unable to provide exact quantification of activity amounts but provide a measurement of qualitative purity assessment. The γ-counter can provide quantitative activity amounts for the radioisotope of interest and the impurity, and is also broadly available, leading to the possibility for more accurate and accessible quality control of complex-emitting radiopharmaceuticals.

Conclusion

The development and clinical evaluation of ^{227}Th and ^{223}Ra therapies place new demands on radiochemists and pharmacists to ensure safe and effective use. As the field evolves to regulate and handle these potent agents, the authors have investigated widely deployed, robust, and affordable methods for their quality control.[16] The data demonstrate an accessible method for assessing ^{227}Th and ^{223}Ra radiopharmaceutical purity using a γ-counter after discrimination of each isotope.

Radio-TLC and α-particle spectrometer imaging may prove useful for evaluating constituents and purity of a sample, but they may not be ideally suited for evaluation of complex mixtures of isotopes. Overall, this evaluation of two emerging radionuclides for α-therapy treatment underlines technological developments toward improved quality assurance for radiopharmaceuticals with concatenated decays and complex emission profiles.

Authors' Contributions

A.H. contributed to writing (lead), conceptualization (lead), formal analysis (lead), methodology development (equal), review, and editing (equal). W.J. was involved in writing (support), formal analysis (support), methodology development (support), review, and editing (equal). N.B. and L.S. carried out methodology development (support). P.L. carried out methodology development (equal). M.S.L. was involved in conceptualization (support), methodology development (equal), review, and editing (equal). B.J.B. carried out methodology development (equal), review, and editing (equal). H.Z. was in charge of conceptualization (support) and methodology development (support). R.L.W. carried out conceptualization (support), review, and editing (support). D.S.A. took care of writing (equal), conceptualization (lead), formal analysis (equal), methodology development (equal), review, and editing (equal). D.L.J.T. was in charge of writing (equal), conceptualization (equal), formal analysis (equal), methodology development (equal), review, and editing (equal).

Disclosure Statement

There are no existing financial conflicts.

Funding Information

The study herein was funded in part by the National Cancer Institute at the National United States Institutes of Health R01CA229893 (D.L.J.T.), R01CA201035 (D.L.J.T.) and R01CA240711 (D.L.J.T.). Isotopes used in this research were supplied in part by the United States Department of Energy Office of Science, Isotope Program, Office of Nuclear Physics.

Supplementary Material

Supplementary Data
Supplementary Figure S1
Supplementary Figure S2

References

1. Den RB, George D, Pieczonka C, et al. Ra-223 treatment for bone metastases in castrate-resistant prostate cancer: Practical management issues for patient selection. Am J Clin Oncol 2019;42(4):399–406; doi: 10.1097/COC.0000000000000528
2. Poeppel TD, Handkiewicz-Junak D, Andreeff M, et al. EANM guideline for radionuclide therapy with radium-223 of metastatic castration-resistant prostate cancer. Eur J Nucl Med Mol Imaging 2018;45(5):824–845; doi: 10.1007/s00259-017-3900-4
3. Abou DS, Ulmert D, Doucet M, et al. Whole-body and microenvironmental localization of radium-223 in naïve and mouse models of prostate cancer metastasis. J Natl Cancer Inst 2016;108(5):djv380; doi: 10.1093/jnci/djv380
4. Parker C, Heinrich D, Helle SI, et al. Alpha emitter Radium-223 and survival in metastatic prostate cancer. N Engl J Med 2013;369:213–223; doi: 10.1056/NEJMoa1213755
5. Jiang W, Ulmert D, Simons BW, et al. The impact of age on radium-223 distribution and an evaluation of molecular imaging surrogates. Nucl Med Biol 2018;62–63:1–8; doi: 10.1016/j.nucmedbio.2018.05.003
6. Ramdahl T, Bonge-Hansen HT, Ryan OB, et al. An efficient chelator for complexation of thorium-227. Bioorg Med Chem Lett 2016;26(17):4318–4321; doi: 10.1016/j.bmcl.2016.07.034
7. Larsen RH, Borrebaek J, Dahle J, et al. Preparation of ^{227}Th labeled radioimmunoconjugates, assessment of serum stability and antigen binding ability. Cancer Biother Radiopharm 2007;22(3):431–437; doi: 10.1089/cbr.2006.321
8. Liberal FDC, O'Sullivan JM, McMahon SJ, et al. Targeted alpha therapy: Current clinical applications. Cancer Biother Radiopharm 2020;35(6):404–417; doi: 10.1089/cbr.2020.3576
9. Bruland O, Nilsson S, Fisher DR, et al. High-linear energy transfer irradiation targeted to skeletal metastases by

the α-Emitter ^{223}Ra: Adjuvant or alternative to conventional modalities? Clin Cancer Res 2006;12(20):6250s–6257s; doi: 10.1158/1078-0432.CCR-06-0841
10. Smith T, Kearfott KJ. Practical considerations for gamma ray spectroscopy with NaI(Tl). Health Phys 2018;114(1):94–106; doi: 10.1097/HP.0000000000000804
11. Marcus CS. How should the FDA review diagnostic radiopharmaceuticals? J Nuclear Med 2018;59(6):868–870; doi: 10.2967/jnumed.117.200337
12. Schwarz SW, Clarke B. Perspective on how the FDA should review diagnostic pharmaceuticals. J Nuclear Med 2018;59(6):865–867; doi: 10.2967/jnumed.117.204446
13. Abou DS, Pickett J, Mattson JE, et al. A Radium-223 microgenerator from cyclotron-produced trace Actinium-227. Appl Radiat Isot 2017;119:36–42; doi: 10.1016/j.apradiso.2016.10.015
14. Bateman H. The solution of a system of differential equations occurring in the theory of radioactive transformations. Proc Cambridge Phil Soc 1910;15(V):423–427.
15. Assessment Report—Xofigo®. European Medicines Agency. 2013. Available from: https://www.ema.europa.eu/en/documents/assessment-report/xofigo-epar-public-assessment-report_en.pdf [Last accessed October 2021].
16. Hagemann UB, Wickstroem K, Hammer S, et al. Advances in precision oncology: Targeted Thorium-227 conjugates as a new modality in targeted alpha therapy. Cancer Biother Radiopharm 2020;35(7):497–510; doi: 10.1089/cbr.2020.3568